

# **influence of scanning speed on the intermetallic produced in-situ in laser metal deposited TiC/Ti6Al4V composite**

**Rasheedat M. Mahamood<sup>a,b\*</sup> and Esther T. Akinlabi<sup>a</sup>**

<sup>a</sup> University of Johannesburg, Auckland Park, Kingsway Campus, Johannesburg, 2006, South Africa

<sup>b</sup>University of Ilorin, Tanke road, 23400003, Nigeria.

\*Corresponding Author: [Email-mahamoodmr2009@gmail.com](mailto:Email-mahamoodmr2009@gmail.com)

## **Abstract**

Effect of scanning speed on titanium aluminide-Ti<sub>3</sub>Al produced in-situ during laser metal deposited TiC/Ti6Al4V has been investigated and its effect on microhardness and wear resistance properties has been studied. In this study, titanium alloy –Ti6Al4V (an important aerospace alloy) was deposited in combination with titanium carbide-TiC using laser metal deposition process. The laser power was maintained at 3.2 kW throughout the deposition process. The powder flow rate and the gas flow rate were also kept at constant values of 2.88 g/min and 2 l/min respectively. The scanning speed was varied between 0.015 and 0.105 m/s , and the influence of the scanning speed on the titanium aluminide (Ti<sub>3</sub>Al) produced in-situ was studied and its effect on the wear resistance behaviour was also investigated. The study revealed that as the scanning speed was initially increased, the Ti<sub>3</sub>Al produced in-situ was found to increase and the wear resistance was found to improve. As the scanning speed was further increased beyond 0.06 m/s, the Ti<sub>3</sub>Al produced and the wear resistance were found to decrease.

*Keywords: Laser Metal Deposition process; Microhardness; Microstructure; Titanium alloy; Ti<sub>3</sub>Al; Wear resistance*

## **1 INTRODUCTION**

Ti6Al4V is widely used in industries because of its good combination of properties, such as high specific strength, low density and good corrosion resistance. However, Ti6Al4V has poor wear resistance property owing to their chemical behaviour that tends to reduce its further application.<sup>1</sup> <sup>2</sup> The surface property of the material can be modified in order to improve its wear resistance property. Different surface treatment methods have been applied to titanium alloy in order to improve their wear resistance property in the literature such as physical vapor deposition process, chemical vapor deposition process and sol-gel methods.<sup>3, 4</sup> The laser metal deposition (LMD) process, an additive manufacturing technique is more advantageous of all other methods. This is because, complex shaped part can be produced with the desired surface properties directly from the three dimensional (3D) computer aided design (CAD) model of the part by adding material layer by layer.<sup>5</sup> LMD also has the flexibility of handling more than one material simultaneously, thereby making it possible to make part with composite or functionally graded materials.

An intermetallic compound of Ti<sub>3</sub>Al have been found to have several advantages such as, higher elastic modulus, lower density, better mechanical properties at elevated temperatures and higher oxidation resistance because it forms a surface passivated alumina layer.<sup>1</sup> The intermetallic-matrix

composites (IMCs) with ceramic particles are also found to possess higher specific strength, improved toughness, and high temperature strength retention.<sup>6, 7</sup> A lot of studies have been conducted in the literature on intermetallic compound reinforced ceramic composite as a result of the improved properties they offer.<sup>8-10</sup> In this work, a composite of TiC/Ti6Al4V was produced and Ti<sub>3</sub>Al was formed in-situ. The effect of scanning speed on the quantity of the Ti<sub>3</sub>Al formed in-situ was studied and its influence on the microhardness and the wear resistance properties were investigated in detail and reported.

## 2 EXPERIMENTAL TECHNIQUE

The powders used in this study are titanium alloy-Ti6Al4V power of 99.6 % purity, supplied by VSMPO-AVISMA Corporation, Russia and TiC powder of 99.5% purity and it was supplied by F.J. Brodmann and Co., L.L.C., Louisiana. The substrate material used is a 99.6% pure Ti6Al4V, 72 x 72 x 5 mm sheet. The chemical compositions of the powders and the substrate are listed in **Table I**. The TiC powder is of particle size range below 60 µm and the Ti6Al4V powder is of particle size range between 150 and 200 µm. The substrate was sandblasted and then degreased using acetone before the deposition processes: this is to improve the laser energy absorption. A Kuka robot was used for the laser metal deposition experiment. The 4.0 kW Nd-YAG laser (Rofin Sinar) was attached to the robot's end effector with two coaxial powder delivery nozzles. The experimental set-up also consist of a glove box, a table and a two-hoppers powder feeder. The experimental set-up is shown in **Figure 1**. The two powders were put in a separate hopper of the powder feeder and the powder flow rates were set at the setting to give 50 W% of TiC powder and 50 W% Ti6Al4V powder for the composite. Multiple tracks were produced at 50 % overlap. The laser power was set at 3.2 kW and maintained at that value throughout the deposition process. The

powder flow rate and the gas flow rate were set and kept at constant values of 2.88 g/min and 2 l/min respectively. The scanning speeds were varied between 0.015 and 0.105 m/s. The Argon gas was used to keep the oxygen level in the glove box below 10 ppm during the deposition process to prevent the atmospheric oxygen and nitrogen from contaminating the deposits. The laser metal deposition process was achieved by feeding the powders through the coaxial nozzles into the melt pool that was created on the substrate by the laser beam which forms the composite after the solidification of the melt pool. See **Figure 2** for the schematic of the laser metal deposition process.

Scanning electron microscopy (SEM), X-ray energy-dispersive spectroscopy (EDS) analysis, and X-ray diffraction (XRD) were used for microstructures and phase analyses of the deposited samples respectively. Samples for the SEM and microhardness were sectioned laterally, mounted in hot resin, ground and polished using the standard metallographic techniques according to the ASTM E3 – 11, standard.<sup>11</sup> The SEM samples were etched using the Kroll's reagent. The Kroll's reagent consists of 100 ml of water with 2 ml of hydrofluoric acid and 4 ml of nitric acid. The microhardness measurements were conducted using a Vickers indenter under a 300-g load and a dwelling time of 15s according to ASTM E384 - 11e1 (2011) standard.<sup>12</sup> The wear tests were performed under the dry condition (no lubrication) using a ball on disk arrangement on a Cert tribotester. A Tungsten Carbide ball of 10 mm diameter was used at a load of 25 N, reciprocating frequency of 20 Hz and at a sliding distance of 2000 mm. The wear test was performed according to the ASTM G133 – 05(2010) Standard<sup>13</sup>

<insert Table 1>

<insert Figure 1>

<insert Figure 2>

### 3 RESULTS AND DISCUSSION

The morphologies of the Ti6Al4V and TiC powders are shown in **Figures 3 (a) and (b)** respectively. The micrograph of the Ti6Al4V substrate is shown in Figure 3c. The Ti6Al4V powder is characterized by spherically shaped powder particles which is typical of a gas atomized powder.<sup>15</sup> Spherically shaped gas atomized powder is more favoured in laser metal deposition process because of its improved absorption of the laser rays.<sup>15</sup> The TiC powder is a ball milled powder with irregular shape which is the characteristics of any ball milled powder. The Ti6Al4V substrate is characterized by alpha (light contrast) and beta (dark contrast) phase as shown in **Figure 3 (c)**.

<insert Figure 3>

The results of the intermetallic of Ti<sub>3</sub>Al (in percentage), the average Vicker's hardness number and the wear volume loss are presented in **Table 2**.

<insert Table 2>

The graph of the  $\text{Ti}_3\text{Al}$  intermetallic against the scanning speed is shown in **Figure 4 (a)**. The graph of the average Vicker's hardness against the scanning speed is shown in **Figure 4 (b)**. The wear volume is plotted against the scanning speed and is shown in **Figure 4 (c)**. The combined graph of the  $\text{Ti}_3\text{Al}$  intermetallic and the wear volume is shown in **Figure 4 (d)**. The  $\text{Ti}_3\text{Al}$  intermetallic was found to increase as the scanning speed was initially increased. The maximum  $\text{Ti}_3\text{Al}$  intermetallic was seen at the scanning speed of 0.065 m/s with a value of 15%. As the scanning speed was increased beyond 0.065 m/s, the  $\text{Ti}_3\text{Al}$  intermetallic was seen to start decreasing. Our earlier study also revealed that as the scanning speed was increased, the wear resistance was found to be increased and then decrease as the scanning speed was further increased. The reason for this was attributed to the unmelted carbide (UMC) particles whose size and quantity was found to be responsible for the wear behaviour of the laser metal deposited TiC/Ti6Al4V composite.<sup>16</sup> The present investigation shows that it was not only the unmelted carbide particles that were responsible for the wear resistance behaviour, the  $\text{Ti}_3\text{Al}$  intermetallic formed also contributed to it. The XRD analysis (see **Figure 5**) revealed that the  $\text{Ti}_3\text{Al}$  intermetallic was changing with the change in the scanning speed and it is also found to have effect on the wear resistance behaviour as shown in the **Figure 4 (a)**. The higher quantity of  $\text{Ti}_3\text{Al}$  intermetallic was seen to improve the wear resistance behaviour of the TiC/Ti6Al4V composites. The  $\text{Ti}_3\text{Al}$  intermetallic is formed as a result of the solid state phase transformation of the primary  $\alpha$  phase structure at low scanning speed. At low scanning speed, the laser material interaction time is longer and the melt pool created is larger thereby causing the solidification and cooling time to be longer and thus allowing low quantity of the  $\text{Ti}_3\text{Al}$  to be formed. As the scanning speed was increased, the laser material interaction time was reduced and the melt pool produced is smaller. This promotes the rapid solidification and the cooling rate of the melt pool that favours larger

quantity of the  $\text{Ti}_3\text{Al}$  to be formed. As the scanning speed was further increased beyond 0.065 m/s the percentage  $\text{Ti}_3\text{Al}$  is found to be reduced. This may be because of improper melting of the TiC powder at these higher scanning speeds. If the scanning speed is too large, the laser material interaction time will be very short and this may result in improper melting of the powders. Also, because the melt pool created at such high scanning speeds are very small will resulting in the formation of low quantity of the  $\text{Ti}_3\text{Al}$  intermetallic. Since intermetallic compound are produced from the solid-state reaction of the solidified melted powders and if the quantity of the melted powder is reduced as a result of high scanning speeds. It follows that the quantity of the  $\text{Ti}_3\text{Al}$  intermetallic formed will be reduced. On the other hand, the microhardness was found to continue to increase as the scanning speed was increased as shown in **Figure 4 (b)**. This is because of the insufficient melting of the TiC powder particles as a result of the low laser material interaction time that resulted in the production of larger unmelted carbide particles. The increase in the microhardness values even at much high scanning speed may be as a result of these unmelted carbide particles. The large particles of the unmelted TiC carbide are detrimental to the wear resistance properties and that is why the wear resistance properties are found to be reducing as the scanning speed was increased beyond 0.065 m/s. The large unmelted TiC particles cause damage to the sliding surface as a result of the cutting and tearing action of these large unmelted TiC particles during the rubbing actions.

<insert Figure 4>

<insert Figure 5>

<insert Figure 6>

Also as shown in the past study that, as the scanning speed was increased, the size and the quantity of the unmelted TiC particles also increased which formed a powder lubricant that inhibit the wear action as the slidding action progresses.<sup>16</sup> The Ti<sub>3</sub>Al also mimic the behaviour of the unmelted carbide action as it is also hard and brittle which also forms powder lubricant as the sliding wear action continues, due to rubbing and gridding of the Ti<sub>3</sub>Al and the unmelted carbide particles (see **Figure 6**) as the wear action continues. The particle size of these Ti<sub>3</sub>Al intermetallic and the smaller unmelted TiC carbide particles are reduced in size as they are rubbed against one another during the wear experiment. These unmelted TiC and the Ti<sub>3</sub>Al intermetallic particles were ground by the rubbing surfaces of the deposited sample and the Tungsten carbide ball to form fine powder. The fine powder now form protective layer between the rubbing surfaces which prevent the two surfaces to be in contact thereby forming a powdery lubricant between the two surfaces and thus, reducing the wear action.

The wear track of the parent material is shown in **Figure 7 (a)**. The wear action of the parent material is characterized by parallel ploughing grooves as shown in **Figure 7 (a)**, and there formation is as a result of the combination of abrasive wear, adhesive wear and plastic deformation.<sup>16</sup> The wear tracks of the samples at 0.015 m/s is shown in **Figure 7 (b)**, that of the sample at a scanning speed of 0.065 m/s is shown in **Figure 7 (c)** and the wear track of the sample at the scanning speed of 0.105 m/s is shown in **Figure 7 (d)**. At low scanning speed, the UMC and the Ti<sub>3</sub>Al seen in the microstructure are less than those seen at higher scanning speed. Both the UMC and the Ti<sub>3</sub>Al serve as reinforcement in the composite. The less quantity of these



reinforcement does not really improve the wear resistance because they are serving as a third body wear mechanism that results in cutting of the surfaces in sliding motion as seen in **Figure 7 (b)**. The size of UMC is smaller at scanning speed of 0.065 m/s when compared to those seen at higher scanning speed. Also, the quantities of the UMC are more than those seen at lower scanning speed where most of the TiC powder is completely melted. The quantity of the Ti<sub>3</sub>Al is also more at the scanning speed of 0.065 m/s thereby resulting in improved wear resistance behaviour (see **Figure 7 (c)**). This is because the UMC particles and the Ti<sub>3</sub>Al are grounded into finer powder as the sliding action progresses as they are hard and brittle. The powder they form serves as a protective layer (as powder lubricant) which tends to reduce the wear action of the two surfaces in the sliding motion. The size of the UMC particles seen in the scanning speed of 0.105 m/s is larger than those seen at lower scanning speed because of the lower laser material interaction time at higher scanning speed. There was not enough time to melt the surfaces of the TiC powder particles at higher scanning speed thereby leaving behind larger UMC TiC particles. Also, the quantity of the UMC TiC particles as well as the Ti<sub>3</sub>Al intermetallic is fewer than those seen at the scanning speed of 0.065 m/s. These large UMC TiC particles cause cracking of the surfaces in the sliding motion thereby escalating the wear action as shown in **Figure 7 (d)**.

<insert Figure 7>

#### **4 CONCLUSION**

A study on the influence of scanning speed on the Ti<sub>3</sub>Al intermetallic produced in-situ during laser metal deposition process has been conducted. The scanning speed was varied between 0.015 and 0.105 m/s. The evolving microstructures were studied; microhardness and wear test were also

performed. The effect of the quantity of the  $Ti_3Al$  on the wear resistance property was investigated. Qualitative metallographic analysis of the microstructures confirmed that during the solidification and cooling processes of the deposited samples, the  $Ti6Al4V$  and the  $TiC$  powders were transformed into various phases including intermetallic phase of  $Ti_3Al$ . Also, secondary phase of  $Ti_3Al$  is formed in-situ by chemical reactions between the  $Ti6Al4V$  and the  $TiC$ . The intensive phase transformations that occurred, during the solidification and cooling down process resulted in the various quantity of the  $Ti_3Al$  produced which was found to initially increase as the scanning speed was increased and then reduce as the scanning speed was further increased. The wear test conducted revealed that the wear resistance property initially increased as the scanning speed was increased and then decrease as the scanning speed was increased beyond 0.065 m/s. Also, the maximum  $Ti_3Al$  observed also occurred at the same scanning speed and it was found to be 15%. It can be concluded that, the optimum scanning speed for the best wear resistance performance of laser metal deposited  $Ti6Al4V$  and  $TiC$  composite is 0.065 m/s for the set of other processing parameters considered in this study.

### **Acknowledgments**

This work is supported by L'Oreal UNESCO for Women in Science and University of Johannesburg Research Council

## **5 REFERENCES**

- <sup>1</sup> C. H. J. Hager, J. H. Sanders, S. Sharma, Unlubricated gross slip fretting wear of metallic plasma-sprayed coatings for Ti6Al4V surfaces, *Wear*, 265 (2008) (3/4), 439–451, doi:10.1016/j.wear.2007.11.026
- <sup>2</sup> W. Pang, H. C. Man, T. M. Yue, Laser surface coating of Mo–WC metal matrix composite on Ti6Al4V alloy, *Materials Science and Engineering A*, 390 (2005) (1/2), 144–153, doi:10.1016/j.msea.2004.07.065
- <sup>3</sup> F. Variola, J. H. Yi, L. Richert, J. D. Jwues, F. Rosei, A. Nanci, Tailoring the surface properties of Ti6Al4V by controlled chemical oxidation, *Biomaterials*, 29 (2008 ) (10), 1285–1298, doi:10.1016/j.biomaterials.2007.11.040
- <sup>4</sup> M. M. Silva, M. Ueda, L. Pichon, H. Reuther, C. M. Lepienski, Surface modification of Ti6Al4V alloy by PIII at high temperatures: Effects of plasma potential, *Nuclear Instruments and Methods in Physics Research B*, 257 (2007 ) (1/2), 722–72, doi:10.1016/j.nimb.2007.01.135
- <sup>5</sup> J. Scott, N. Gupta, C. Wember, S. Newsom, T. Wohlers, T. Caffrey, Additive manufacturing: status and opportunities, Science and Technology Policy Institute, (2012). Retrieved 11<sup>th</sup> July 2012, from [https://www.ida.org/stpi/occasionalpapers/papers/AM3D\\_33012\\_Final.pdf](https://www.ida.org/stpi/occasionalpapers/papers/AM3D_33012_Final.pdf)
- <sup>6</sup> L. Cai, Y. Zhang, L. Shi, Microstructure and formation mechanism of titanium matrix composites coating on Ti-6Al-4V by laser cladding, *Rare Metals*, 26 (2007) (4), 342–346, doi:10.1016/S1001-0521(07)60226-5
- <sup>7</sup> J. D. Majumdar, I. Manna, A. Kumar, Direct laser cladding of Co on Ti-6Al-4V with a compositionally graded interface, *Journal of Materials Processing Technology*, 209 (2009) (5), 2237–2243, doi:10.1016/j.jmatprotec.2008.05.017

- <sup>8</sup> R. Mahmoodian, M.A. Hassan, M. Hamdi, R. Yahya, R.G. Rahbari, In situ TiC–Fe–Al<sub>2</sub>O<sub>3</sub>–TiAl/Ti<sub>3</sub>Al composite coating processing using centrifugal assisted combustion synthesis, *Composites Part B: Engineering*, 59(2014), 279-28, doi:10.1016/j.compositesb.2013.12.016
- <sup>9</sup> Z. Liu, X. Zhang, F. Xuan, Z. Wang, and S. Tu, Effect of laser power on the microstructure and mechanical properties of TiN/Ti<sub>3</sub>Al composite coatings on Ti6Al4V, *Chinese Journal of Mechanical Engineering*, 26 (2013) 4, 714-721, doi: 10.3901/CJME.2013.04.714
- <sup>10</sup> B. G. Guo, J. S. Zhou, S. T. Zhang, H. D. Zho, Y. P. Pu, J. M. Chen, Microstructure and tribological properties of in situ synthesized TiN/Ti<sub>3</sub>Al intermetallic matrix composite coatings on titanium by laser cladding and laser nitriding. *Mater Science Engineering A*, 480 (2008), 404–10, doi:10.1016/j.msea.2007.07.010
- <sup>11</sup> E3–11. Standard Guide for Preparation of Metallographic Specimens, ASTM international Book of Standards, 03 (2011) 01, **doi: 10.1520/E0003-11**
- <sup>12</sup> ASTM E92 - 16. Standard Test Method for Vickers Hardness and Knoop hardness of metallic Materials, ASTM International Book of Standards, 03 (2016) 01, doi: 10.1520/E0092-16
- <sup>13</sup> ASTM G133 – 0. Standard Test Method for Linearly Reciprocating Ball-on-Flat Sliding Wear, ASTM International Book of Standards, 03 (2010) 02, doi: 10.1520/G0133-05R10
- <sup>14</sup> R. M. Mahamood, E. T. Akinlabi, M. Shukla and S. Pityana, Characterization of Laser Deposited Ti6A4V/TiC Composite. *Lasers in Engineering*, 29 (2014) (3-4), 197-213, available at: <http://www.oldcitypublishing.com/journals/lie-home/lie-issue-contents/lie-volume-29-number-3-4-2014/lie-29-3-4-p-197-213/>
- <sup>15</sup> C. T. Schade, T. F. Murphy and Chris Walton, Development Of Atomized Powders for Additive Manufacturing, Powder Metallurgy Word Congress, (2014). Accessed on 2<sup>nd</sup> July

2014 available at: <http://www.gkn.com/hoeganaes/media/Tech%20Library/Schade-Atomized%20Powders%20for%20Additive%20Manufacturing%20%281%29.pdf>

<sup>16</sup> R. M. Mahamood, E. T. Akinlabi, M. Shukla and S. Pityana, Scanning Velocity Influence on Microstructure, Microhardness and Wear Resistance Performance on Laser Deposited Ti6Al4V/TiC Composite, Materials and Design, 50 (2013), 656-666, doi:10.1016/j.matdes.2013.03.049

**Table 1.** Chemical composition of the Ti6Al4V substrate, Ti6Al4V powder and TiC powder

<b>Ti6Al4V substrate</b>								
Element	Al	V	Fe	C	N <sub>2</sub>	H <sub>2</sub>	O <sub>2</sub>	Ti
W%	6.42	3.91	0.19	0.008	0.006	0.004	0.155	balance
<b>Ti6Al4V powder</b>								
Element	Al	V	Fe	C	N <sub>2</sub>	H <sub>2</sub>	O <sub>2</sub>	Ti
W %	6.20	3.90	0.18	0.008	0.005	0.005	0.150	balance
<b>TiC Powder</b>								
Element	C	O <sub>2</sub>	N <sub>2</sub>	Fe	Al	Na	Ti	
W %	19.5	0.28	0.4	0.045	0.03	0.026	balance	

**Table 2.** results

<b>Sample Designation</b>	<b>Scanning Speed (m/s)</b>	<b>Ti<sub>3</sub>Al (%)</b>	<b>Average Vicker's Hardness Number</b>	<b>Wear Volume (mm<sup>3</sup>)</b>
A	0.015	5	386	0.098
B	0.025	6	390	0.082
C	0.035	8	420	0.08
D	0.045	12	448	0.07
E	0.055	13	449	0.061
F	0.065	15	460	0.058
G	0.075	12	469	0.071
H	0.085	10	475	0.086
I	0.095	5	489	0.082
J	0.105	4	498	0.1
Substrate	0	0	300	0.178



**Figure 1.** Experimental set-up



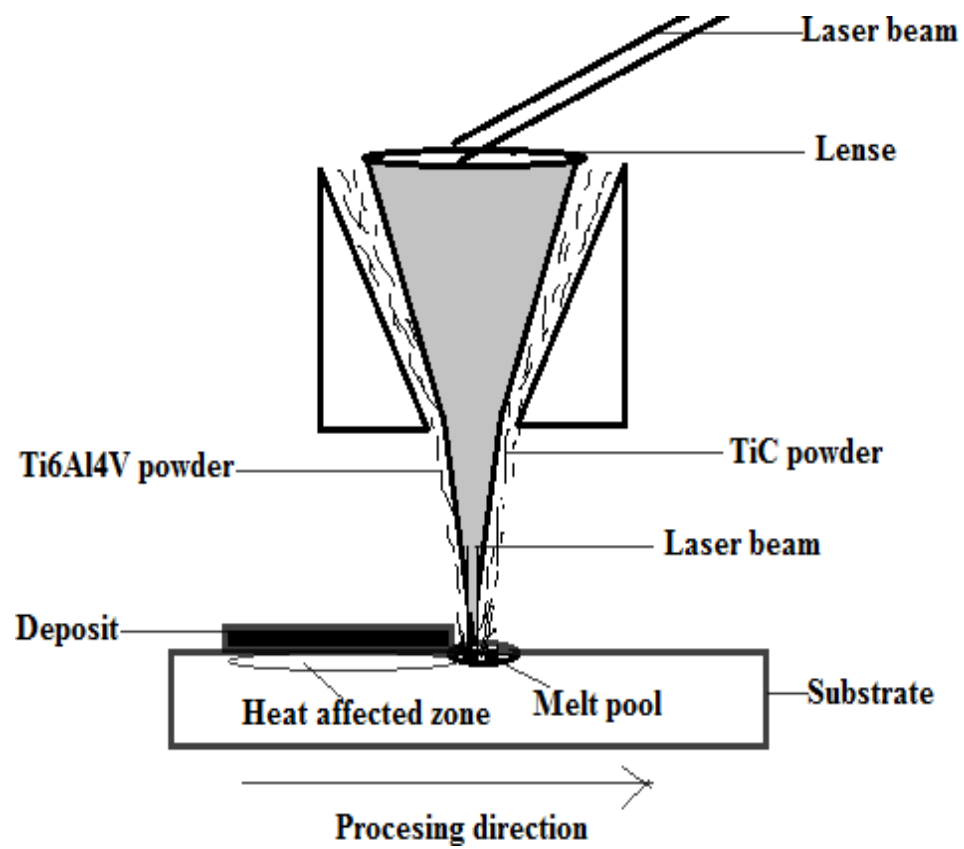
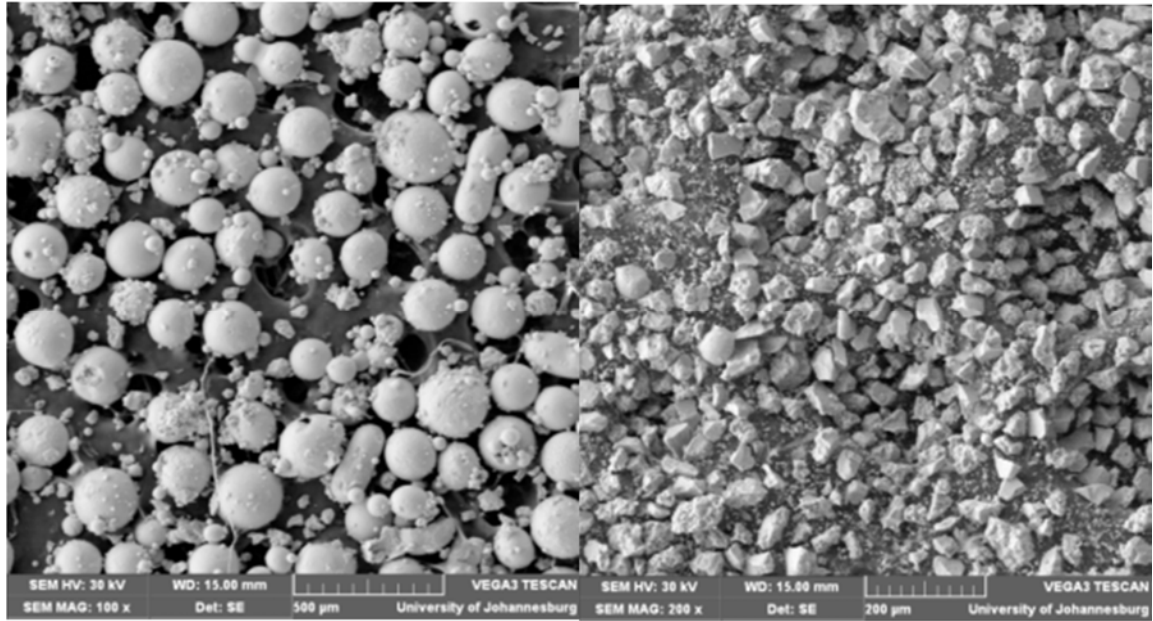
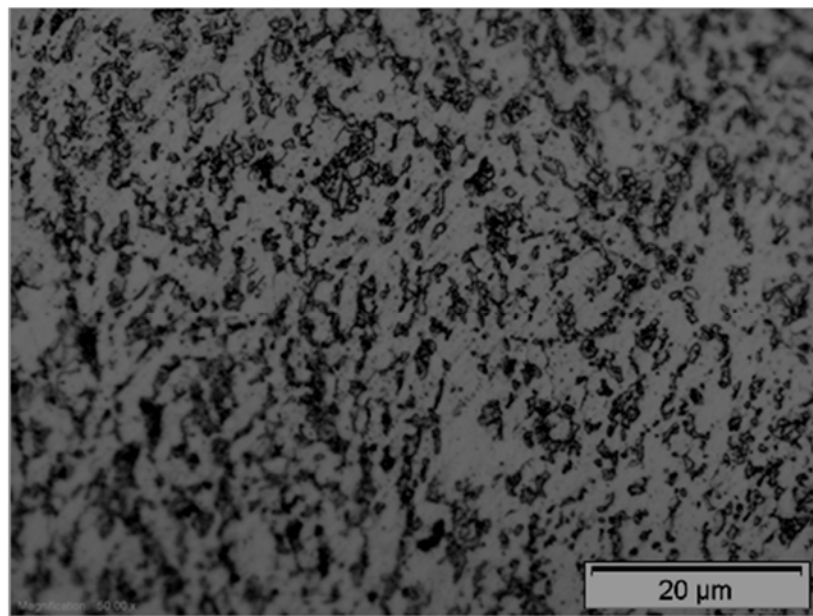


**Figure 2.** the schematic diagram of laser metal deposition process<sup>14</sup>



(a)

(b)



(c)

**Figure 3.** (a) Morphology of the Ti6Al4V powder (b) Morphology of the TiC powder (c) micrograph of the Ti6Al4V substrate

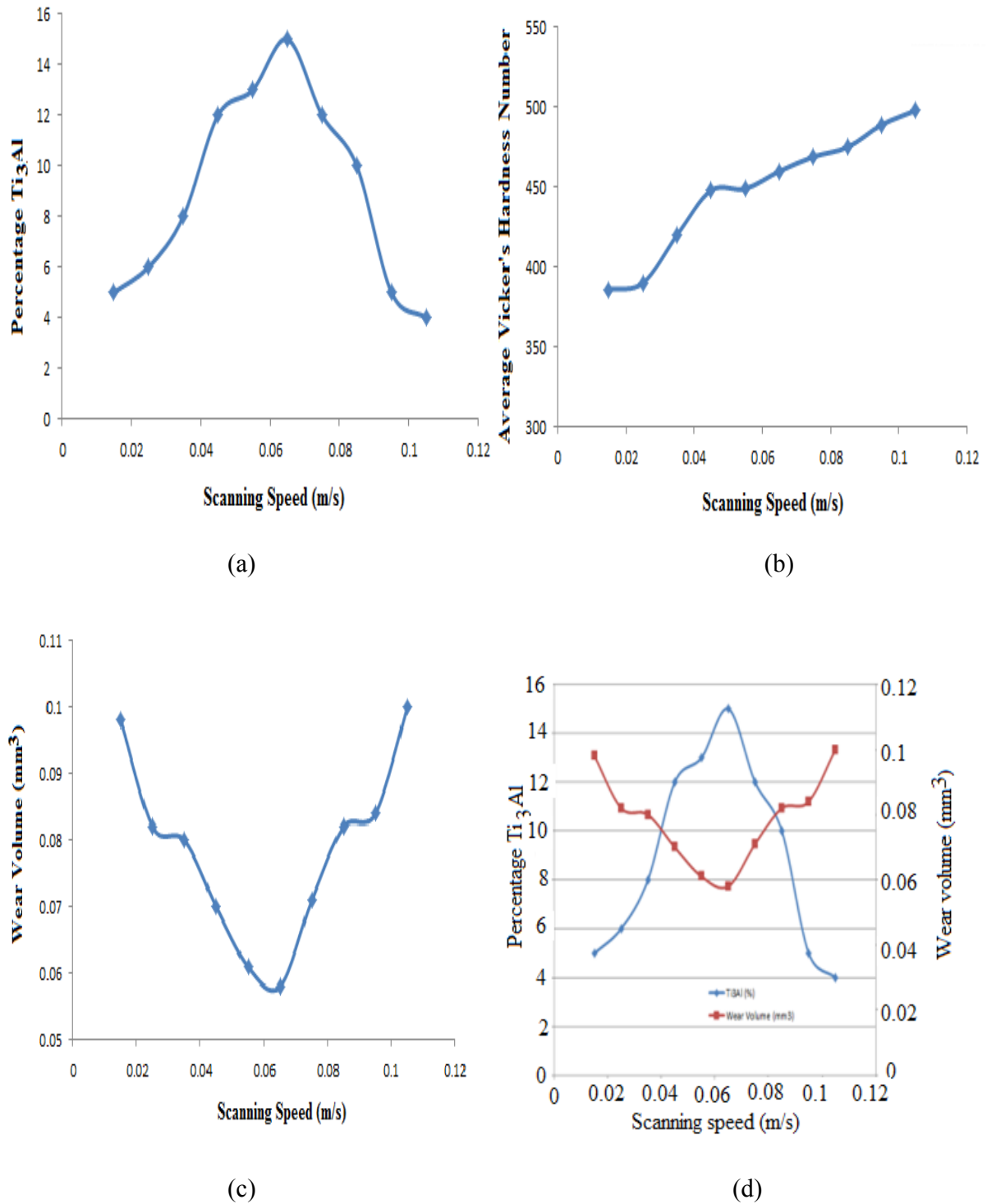
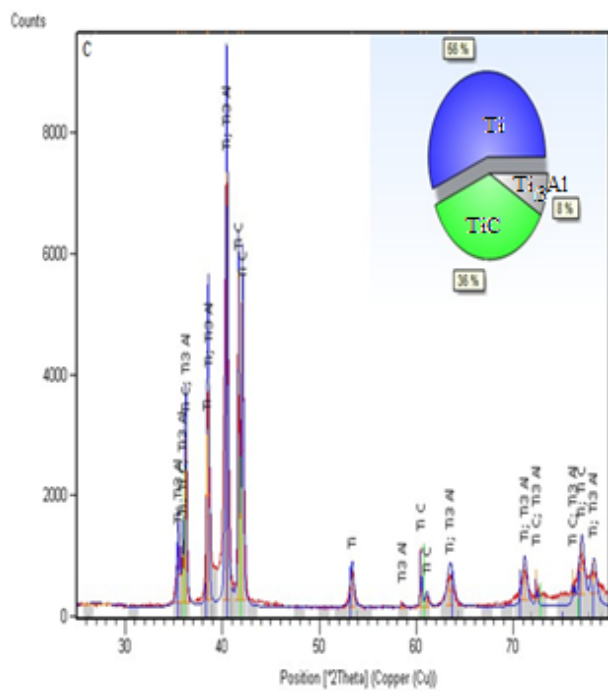
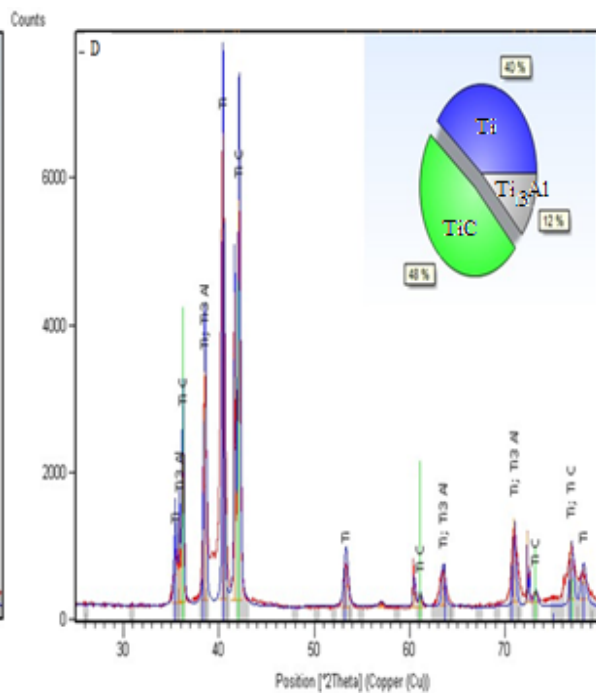


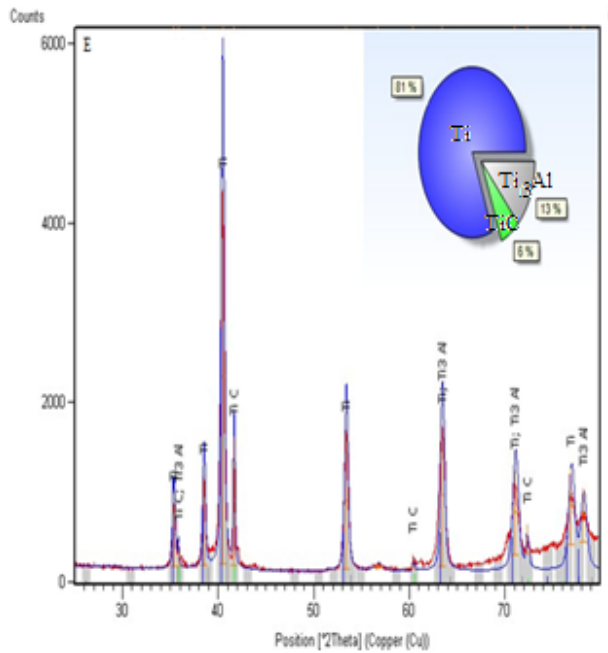
**Figure 4.** the graph of scanning speed and (a) percentage  $Ti_3Al$  (b) average Vicker's hardness (c) wear volume. (d) percentage  $Ti_3Al$  and wear volume.



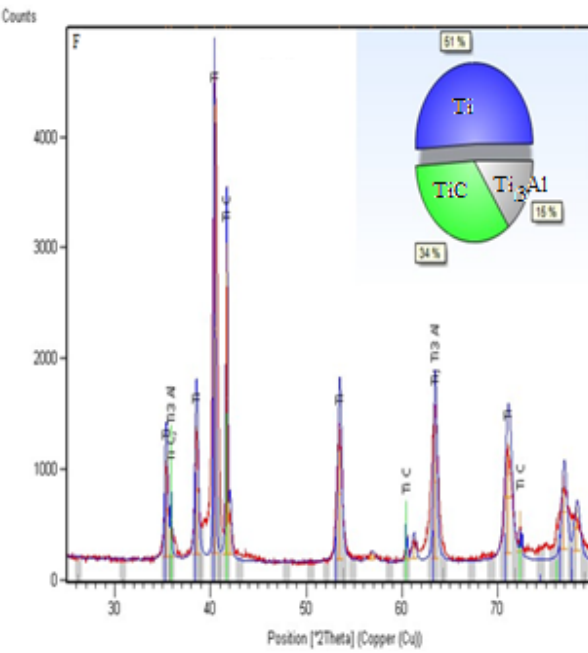
(a)



(b)

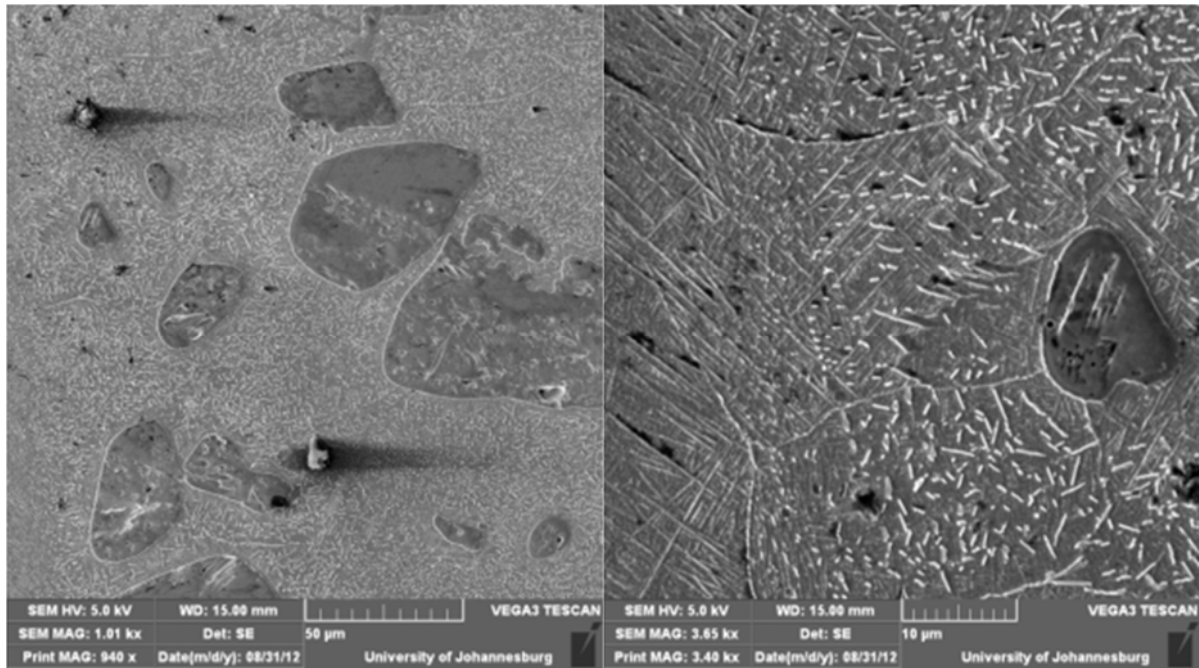


(c)



(d)

Figure 5. The XRD analysis of the sample at the scanning speed of (a) 0.035(b) 0.045 (c) 0.055 (d) 0.065



(a)

(b)

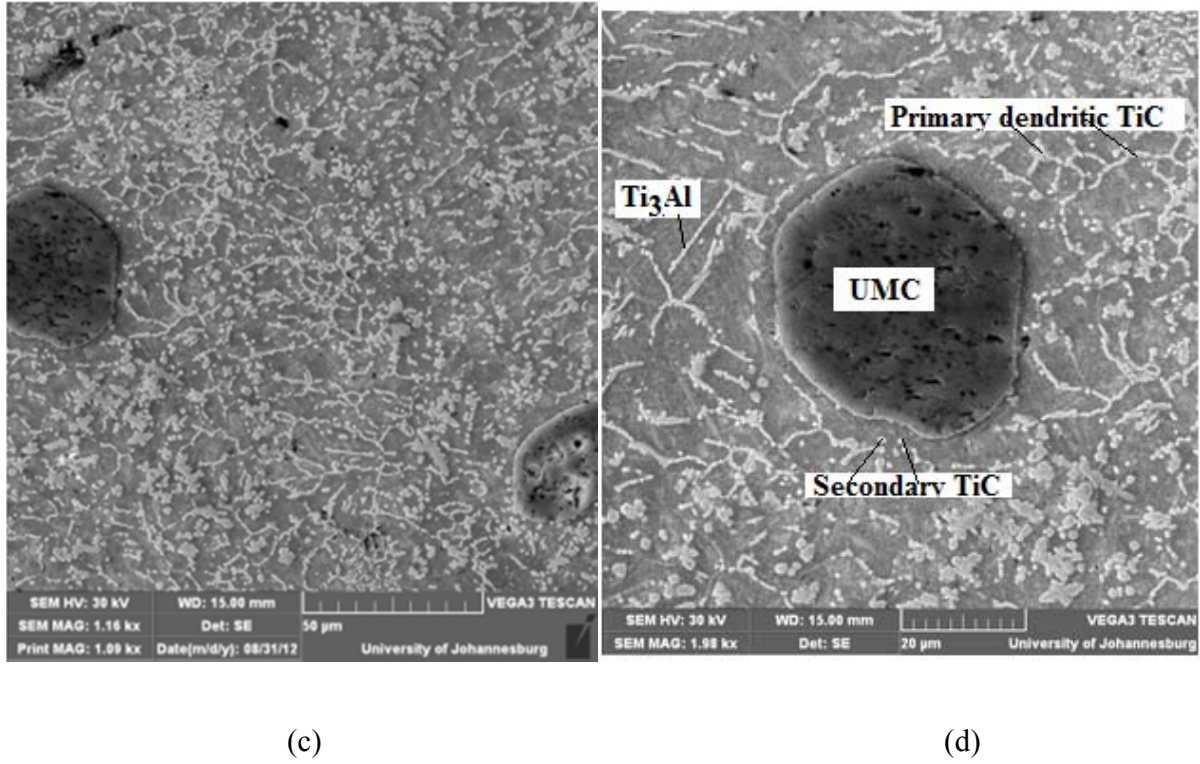
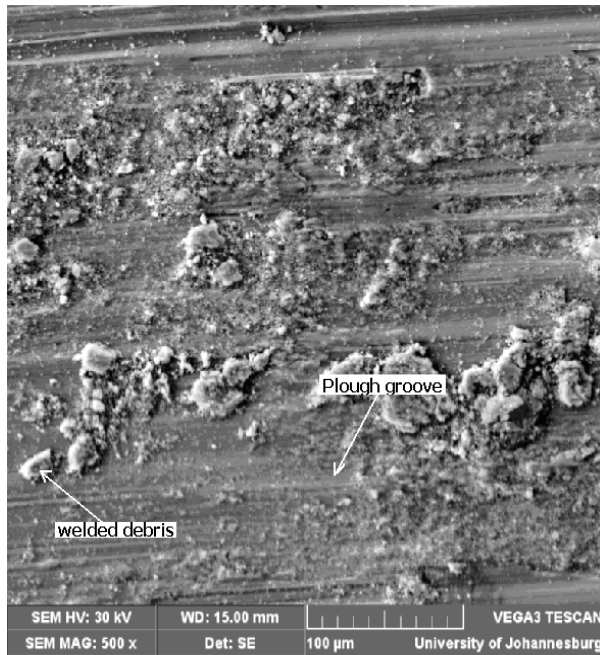
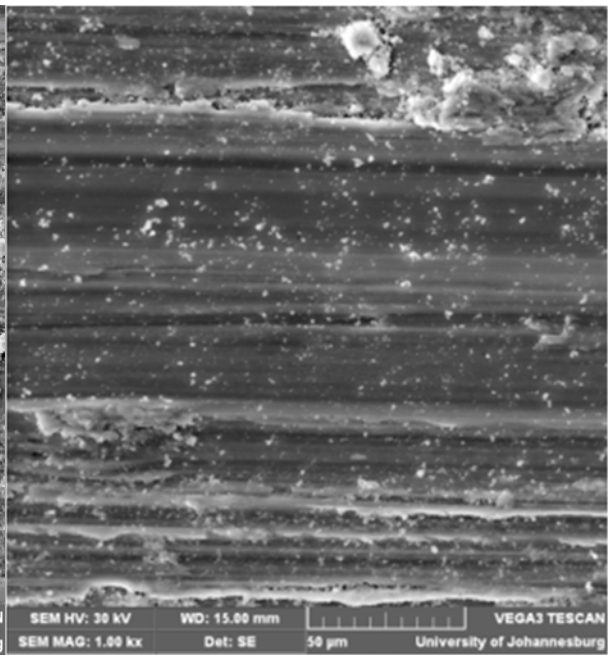


Figure 6. the SEM micrograph of the sample at (a) 0.025 m/s (b) higher magnification of sample in (a). (c) 0.065 m/s (d) higher magnification of sample in (c).

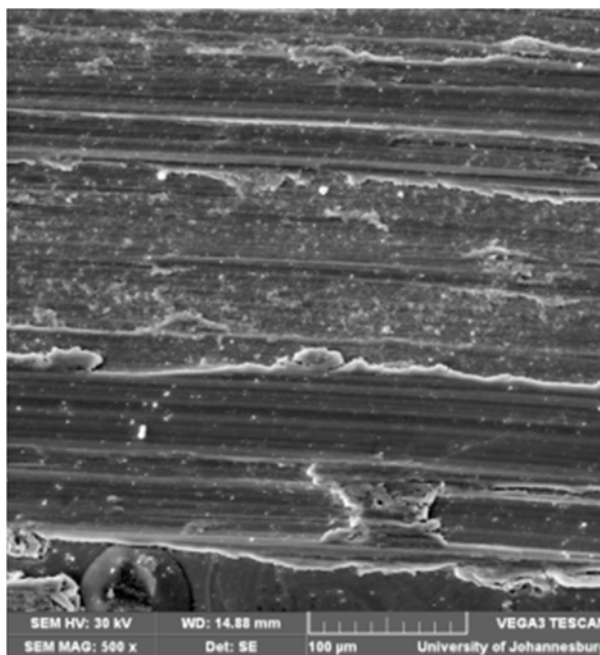




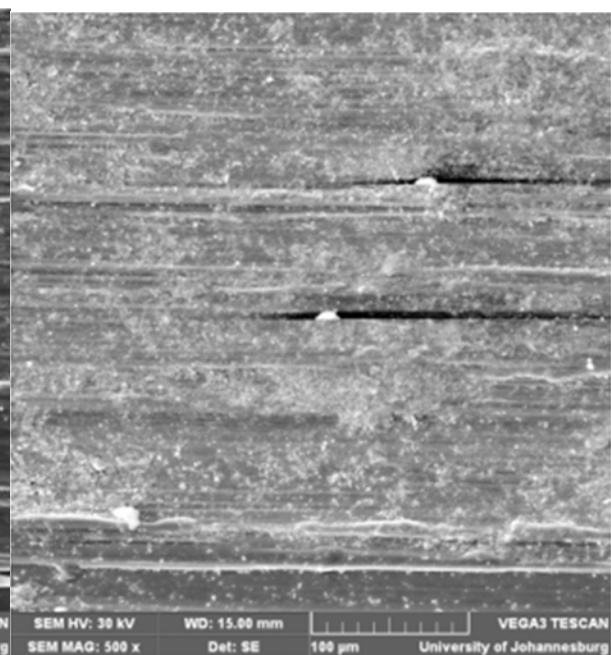
(a)



(b)



(c)



(d)

Figure 7. The SEM micrograph of the wear track of the (a) substrate [16] (b) sample at the scanning speed of 0.015 m/s (c) sample at the scanning speed of 0.065 m/s (d) sample at the scanning speed of 0.105 m/s